Demonstration of spatially inhomogeneous vector beams with elliptical symmetry

Gilad M. Lerman,[1,2] Yigal Lilach,[1] and Uriel Levy[1,*]

[1]*Department of Applied Physics, The Benin School of Engineering and Computer Science, and the Center for Nanoscience and Nanotechnology, The Hebrew University of Jerusalem, Jerusalem 91904, Israel*
[2]*gilad.lerman@mail.huji.ac.il*
**Corresponding author: ulevy@cc.huji.ac.il*

Received February 12, 2009; revised April 19, 2009; accepted April 22, 2009;
posted April 24, 2009 (Doc. ID 107528); published May 27, 2009

We experimentally demonstrate vector beams having an elliptical symmetry of polarization, breaking the cylindrical symmetry of vector beams (e.g., radially polarized beams). Applications of such beams vary from material processing, lithography, and optical memories to excitation of elliptically shaped nanoparticles and plasmonic structures. © 2009 Optical Society of America

OCIS codes: 260.5430, 350.5730, 180.0180.

Following the quest for miniaturization, tight focusing of light is becoming an essential demand. In tight focusing scenarios the vectorial nature of light is affecting the resolution of optical systems [1]. It was shown that under such conditions vector beams perform differently compared with linearly/circularly polarized beams [2–14]. Previous works demonstrated the generation of vector beams holding a cylindrical symmetry. Here we experimentally demonstrate the generation of vector beams with polarization field that follows the direction of concentric ellipses in space—thus providing a new degree of freedom by choosing the ellipses's eccentricity.

In a previous paper [15] we suggested a new type of vector fields that are linearly polarized along an elliptical direction, i.e., the polarization vector of the electric field forms a set of concentric ellipses with constant eccentricity in space. The polarization vector can be chosen to follow a direction perpendicular or parallel to the ellipses (generalization of radially and azimuthally polarized light, respectively). We define these two polarization states as linearly polarized with elliptical radial symmetry (LIPERS) and linearly polarized with elliptical azimuthal symmetry (LIPEAS). The eccentricity ε of these fields can be varied from 0 (equivalent to radial or azimuthal polarization) to 1, thus providing an additional degree of freedom allowing one to control the optical field properties at the focal plane. Schematic representations of LIPERS and LIPEAS fields with $\varepsilon=0.85$ are shown in Figs. 1(a) and 1(b), respectively.

Under tight focusing conditions, the longitudinal component of the electric field is not negligible. By generalizing the method of Richards and Wolf [16] we can calculate the focal plane intensity distribution of any arbitrary polarization distribution impinging on the lens [15]. Our simulations show a strong dependence between the eccentricity of the LIPERS or LIPEAS input field and the intensity distribution near the focal plane. Varying the eccentricity of the input LIPERS field from 0 to 1 results in a transition of the focal plane intensity distribution from a single spot into two separate lobes, as shown in Fig. 2. The interplay between eccentricity and the NA can thus provide a powerful tool in controlling the intensity distribution at the focal plane. As an example, a line of constant intensity, i.e., a narrow spot having flattop intensity distribution along one of its axes, is feasible. Such a pattern is desired for various applications, e.g., material processing. Another application is the excitation of elliptically shaped nanoparticles. Finally, the LIPERS field may become useful for the excitation of plasmonic devices having an elliptical symmetry, similar to the excitation of cylindrically symmetric plasmonic lenses by radially polarized light [17].

Polarization transformation is obtained by the use of subwavelength gratings (SGs), generating π phase retardation between the TE and TM components of the incident beam. By varying the orientation of the SGs one can rotate the polarization at any coordinate across the beam's cross section, creating an electromagnetic field with any desired space variant polarization. By taking $\theta(x,y)$ as the desired local polarization angle with respect to the $\hat{x}$ axis, and assuming an incident beam that is linearly polarized along the $\hat{x}$ axis, the **K** vector of the SGs should be oriented at an angle of $\theta(x,y)/2$ to rotate the incident polarization into the desired elliptical direction. The **K** vector is thus described by

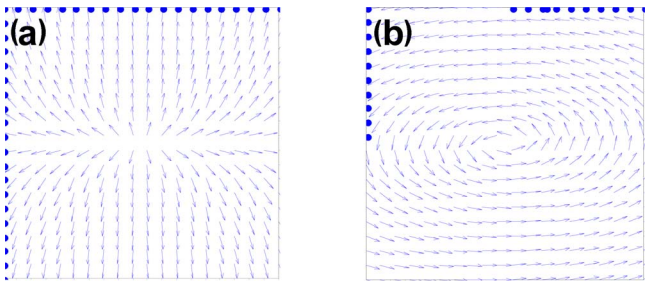

Fig. 1. (Color online) Schematic representations of LIPERS and LIPEAS polarization fields with $\varepsilon=0.85$. The arrows represent the polarization direction at each point. (a) LIPERS polarized field. (b) LIPEAS polarized field.

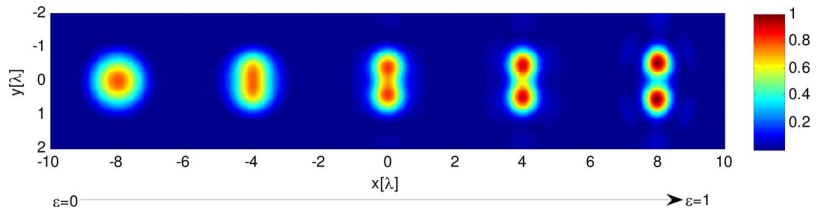

Fig. 2. (Color online) Focal plane intensity distribution of the LIPERS input field with increasing eccentricity. From left to right the eccentricity has the values of 0, 0.6, 0.8, 0.9, and 0.99. All the intensity distributions are normalized by the maximal value of these distributions. The adiabatic transformation of the focal plane intensity distribution from one spot into two separate lobes is clearly observed. The combination of the eccentricity of the input field and the NA of the lens can yield a desired intensity distribution.

$$\vec{k}_g(x,y) = \frac{2\pi}{\Lambda}\left[\cos\left(\frac{\theta(x,y)}{2}\right)\hat{x} + \sin\left(\frac{\theta(x,y)}{2}\right)\hat{y}\right], \quad (1)$$

where Λ is the period of the gratings and $\theta(x,y)$ is found from the ellipse equation.

To implement the polarization converter at a wavelength of $\lambda = 1064$ nm we used a GaAs substrate with a refractive index of $n = 3.478$. We chose the grating period to be 240 nm, which is below the λ/n limit. We divided our polarization transforming device into discrete segments. The SG in each segment was rotated by a half of a degree with respect to the grating in the adjacent segment. This very fine segmentation results in a negligible error in polarization orientation.

The grating patterns were written in an electron beam resist (ZEP 520A) using an electron beam tool (Raith e-line) at 20 kV. We blocked the central portion of the element ($\sim$1% of the whole area), where there was a technological difficulty in writing the SG, by depositing a 150 nm Ag layer on it. The radius of the whole device is 500 μm. The pattern was then transferred into the GaAs substrate using reactive ion etching. Details regarding the etching depth and profile for achieving π phase retardation were reported in [18].

We fabricated a few polarization transformers generating fields with different eccentricities (one can change the output field from LIPERS to LIPEAS by rotating the device by 90°). To record the far-field intensity distributions of the polarized fields we illuminated the devices by a collimated linearly polarized Nd-YAG laser beam (1064 nm wavelength). After passing through the polarization transformer device, the beam was focused by a lens such that the Fourier transform of the spatially inhomogeneous polarized light is obtained at the back focal plane of the lens. The obtained Fourier transform was then captured by a CCD camera. Figure 3 shows the obtained intensity distribution across the Fourier plane for the LIPERS field with eccentricities of 0.79, 0.87, and 0.935 along with the calculated intensity distributions. One can observe a transition toward two distinct lobes as the eccentricity is increased. This can be attributed to the fact that when the eccentricity is increased, the polarization field is approaching a state of a linearly polarized light, except with a π phase shift between the upper and the lower halves of the beam, resulting in two separated lobes in the far field.

The purity of the polarization field after passing through the polarization transformer device was measured by placing a polarizer behind it to convert the polarization modulation into easily observable intensity modulation. Although the LIPERS and LIPEAS fields are not eigenmodes of the wave equation and thus may vary upon propagation in free space (as they are obtained by the superposition of a tilted plane wave having different propagation constants along the optical axis), the polarization transformer device enables one to force any desired boundary conditions in the plane of the device, resulting in the desired polarization distribution in this plane. The device plane can then be imaged to a detection device. Using this concept, we rotated the analyzer with respect to the device and the images of the resulting intensity distribution at each angle of the analyzer were captured by a CCD camera that was placed at the image plane of the polarization converter element. Figure 4 shows the obtained intensity distributions for several angles of the analyzer. The polarization direction is varying across the cross section of the beam, and thus one can see dark and bright zones corresponding to regions where the polarization is perpendicular or parallel to the polarizer axis, respectively.

The intensity of a radially polarized beam after passing through an analyzer varies as $\cos(\theta)$. The dependence of the intensity of a LIPERS field (after passing through the analyzer) on θ is somewhat more complicated, because unlike the radially polarized beam, when moving along the radial coordinate while keeping the azimuthal angle θ constant, the polarization direction is changing. To quantify this depen-

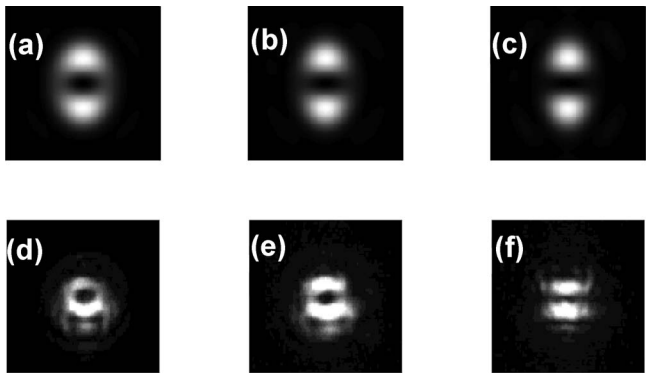

Fig. 3. Far-field intensity distributions for several LIPERS fields. (a)–(c) Computer simulations of LIPERS field with eccentricities of 0.79, 0.87, and 0.935, respectively. (d)–(f) CCD records of the Fourier plane of these polarization fields.

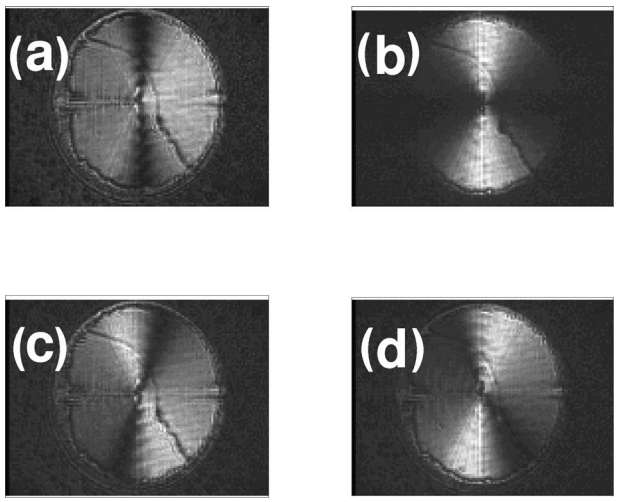

Fig. 4. Mapping of the polarization field by intensity measurement behind a polarizer. The output polarization field from an LIPERS transformer device with $\varepsilon = 0.79$ is imaged onto a CCD camera. A polarizer is put between the device and the camera to convert the polarization distribution into a measurable intensity modulation. (a)–(d) Several angles of the polarizer with respect to the device.

dence we integrated the intensity shown in Fig. 4, along the radial coordinate, between the boundaries of the device's minimal radius (determined by the small opaque area of the device) to its maximal radius, for different values of θ. To compare the obtained results with the theory, we calculated the polarization and the resulting intensity projection on the analyzer direction. For each θ, we integrated the calculated intensities along the radial direction to find the theoretical dependence between the intensity of the LIPERS field after passing through the analyzer and the azimuthal angle θ. Figure 5 shows the theoretical and the experimental normalized results for a polarization rotator device designed for the

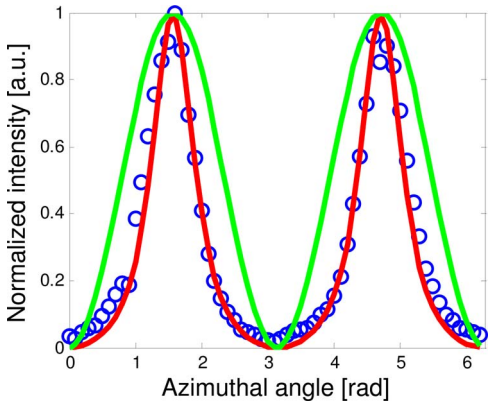

Fig. 5. (Color online) Polarization dependence on the azimuthal angle. The theoretical [red (dark) curve] and experimental (circles) dependences of the polarization of a LIPERS field with an eccentricity of 0.79 on θ—the azimuthal angle. The experimental results were measured by taking one of the pictures shown in Fig. 4 and integrating its intensity along the radial direction for several values of the azimuthal angle θ. The results are normalized, and the theoretical results for the radially polarized field are shown as well [green (light) curve] for comparison.

eccentricity of 0.79. The theoretical results for the radially polarized field are shown as well for comparison purposes. The results fit very well to the theory, with an extinction ratio of more than 55, indicating a high purity of the polarization field emerging from the device. As expected, the dependence of the LIPERS beam on θ is very different compared with that of the radially polarized beam. This difference is increasing with the increase in the eccentricity of the LIPERS field.

To summarize, we provide what we believe to be the first experimental demonstration of light beams with polarization that is space variant in both Cartesian and cylindrical coordinate systems. Specifically, we generated light beams with polarization following the direction of concentric ellipses. The eccentricity of the polarization field provides an additional degree of freedom assisting in controlling the field properties at the focus and allowing for matching the field distribution to the specific application. Potential applications vary from lithography and optical storage to particle beam trapping, material processing, and excitation of elliptically shaped nanoparticles.

The authors acknowledge the support of the Israeli Science Foundation, the Israeli Ministry of Science, Culture and Sport, and the Peter Brojde Center for Innovative Engineering and Computer Science. G. M. Lerman acknowledges financial support from the Eshkol fellowship. Fabrication was supported by the facilities of the Unit for Nanofabrication of the Hebrew University.

References

1. K. A. Serrels, E. Ramsay, R. J. Warburton, and D. T. Reid, Nature Photon. **2**, 311 (2008).
2. K. S. Youngworth and T. G. Brown, Opt. Express **7**, 77 (2000).
3. Q. Zhan and J. R. Leger, Opt. Express **10**, 324 (2002).
4. M. R. Beversluis, L. Novotny, and S. J. Stranick, Opt. Express **14**, 2650 (2006).
5. N. Hayazawa, Y. Saito, and S. Kawata, Appl. Phys. Lett. **85**, 6239 (2004).
6. E. Y. S. Yew and C. J. R. Sheppard, Opt. Lett. **32**, 3417 (2007).
7. E. Descrovi, L. Vaccaro, L. Aeschimann, W. Nakagawa, U. Staufer, and H.-P. Herzig, J. Opt. Soc. Am. A **22**, 1432 (2005).
8. G. M. Lerman and U. Levy, Opt. Express **16**, 4567 (2008).
9. S. C. Tidwell, D. H. Ford, and W. D. Kimura, Appl. Opt. **29**, 2234 (1990).
10. Z. Bomzon, G. Biener, V. Kleiner, and E. Hasman, Opt. Lett. **27**, 285 (2002).
11. A. Shoham, R. Vander, and S. G. Lipson, Opt. Lett. **31**, 3405 (2006).
12. S. Quabis, R. Dorn, M. Eberler, O. Glöckl, and G. Leuchs, Opt. Commun. **179**, 1 (2000).
13. R. Dorn, S. Quabis, and G. Leuchs, Phys. Rev. Lett. **91**, 233901 (2003).
14. U. Levy, C. H. Tsai, L. Pang, and Y. Fainman, Opt. Lett. **29**, 1718 (2004).
15. G. M. Lerman and U. Levy, Opt. Lett. **32**, 2194 (2007).
16. B. Richards and E. Wolf, Proc. R. Soc. London Ser. A **253**, 358 (1959).
17. A. Yanai and U. Levy, Opt. Express **17**, 924 (2009).
18. G. M. Lerman and U. Levy, Opt. Lett. **33**, 2782 (2008).